Enhanced Axial Loss of Electrons from a Tandem Mirror Induced by an Alfvén Ion Cyclotron Wave

T. Saito, M. Ichimura, Y. Kiwamoto,* A. Mase, Y. Tatematsu, H. Abe, K. Kajiwara, Y. Kogi, M. Nakamura, S. Umehara, Y. Yoshimura,† and K. Yatsu

Plasma Research Center, University of Tsukuba, Tsukuba City, Ibaraki 305-8577, Japan

(Received 22 June 1998)

Increases in the flux and temperature of end-loss electrons are observed following excitation of an Alfvén ion cyclotron (AIC) mode in the GAMMA 10 tandem mirror. Electron loss power carried to an end wall becomes more than twice as large as that without the AIC mode. The increases in the electron flux and temperature are observed only when the parallel phase velocity of the AIC mode matches with the electron thermal velocity, strongly suggesting that the parallel electron acceleration is due to electron Landau damping of the AIC mode. [S0031-9007(98)08365-3]

PACS numbers: 52.35.Qz, 52.50.Gj, 52.55.Jd

Electron acceleration by using waves of an ion cyclotron range of frequency has been studied for current drive and electron heating in tokamaks, where electron Landau damping is considered to be a basic mechanism [1–4]. Externally excited fast magnetosonic waves have been used in these experiments. In Landau damping, electrons with a parallel velocity nearly equal to the wave phase velocity are resonantly accelerated along a magnetic field line [5]. Therefore, electron acceleration due to Landau damping of ion waves is also very important in mirror devices because it may affect potential formation and possibly enhance electron axial loss. So far in mirror devices, however, electron acceleration by ion waves has not been studied, except for helicon waves with a frequency much higher than an ion cyclotron frequency, $\omega \gg \omega_{ci}$ [6]. While the theoretical study on interaction between helicon waves and electrons is still under way, electron acceleration by helicon waves has been observed in basic experiments [7,8]. Recently, a slow Alfvén ion cyclotron (AIC) wave with $\omega \leq \omega_{ci}$ was spontaneously excited in a central cell of the GAMMA 10 tandem mirror [9–11], and its interaction with electrons has been found. In this Letter, the first observation of parallel electron acceleration by the AIC wave is reported. From the analysis of the transient feature of the electron acceleration, electron Landau damping is attributed to this interaction.

The AIC wave is spontaneously excited in the central cell in GAMMA 10 with hot ions of a large temperature anisotropy. Its interaction with ions has been reported [10]. The AIC wave causes relaxation of the anisotropy of the ion velocity distribution. This Letter shows a resonant interaction between the AIC wave and electrons, and adds a new aspect to the study of the AIC wave. Many electromagnetic waves with a frequency near ω_{ci} are spontaneously excited in a plasma trapped in a mirror configuration including space plasmas [12,13]. This paper reveals the importance of the electron response to these waves.

Observation of electron Landau damping of a slow wave had been claimed in the C stellarator [14]. The slow wave was externally excited and there was a beach resonance of ions. The electron temperature was indirectly estimated from the Spitzer resistivity. Contrary to this experiment, frequencies of the AIC modes are lower than ω_{ci}. There is no resonance with ions, and resonant interaction with electrons can be extracted. We directly detect accelerated electrons at a machine end by making use of the open field configuration of GAMMA 10 and examining the effects of the AIC mode on electrons. Information on the AIC mode obtained with reflectometers [15] and magnetic probes [16] makes it possible to discuss the Landau damping process.

The GAMMA 10 tandem mirror consists of the central cell, two anchor cells located in both ends of the central cell, and two mirror cells connected to the anchor cells [9]. The magnetic field strength at the midplane of the central cell is 0.405 T and the mirror ratio of the central cell is 5. A slow wave with $\omega > \omega_{ci0}$ is excited for ion cyclotron resonance heating by a pair of antennas installed midway between the midplane and the mirror throats of the central cell. The resonance layer is located between the midplane and antenna position. Here, ω_{ci0} is the ion cyclotron frequency at the midplane of the central cell. Ions are perpendicularly heated and magnetically confined near the midplane. The ion temperature $T_\perp$ perpendicular to the magnetic field line attains several keV. Anisotropy defined by the ratio of $T_\perp$ to the temperature $T_\parallel$ parallel to the magnetic field line becomes larger than 10 [17]. The β value of a hot ion plasma is about 1%. The measurements reported here are all done without electron cyclotron resonance heating at a plug region.

End-loss electrons are measured with an electrostatic energy analyzer of a multigrid type installed on an end wall of the vacuum vessel. End-loss electrons enter the analyzer through a small hole on an electrically floating end plate that is located in front of the end wall. The collector current of the analyzer stands for the electron current flowing into the end plate. The electron repeller voltage of the analyzer is swept, and current voltage characteristics of the end loss electrons can be obtained in one shot.

An AIC mode is excited when a drive term $\beta(T_\perp/T_\parallel)^2$ exceeds a threshold value [11]. Its excitation is monitored

by reflectometers [18] and magnetic probes. Usually, the AIC mode has several peaks in the frequency spectrum. The frequency of each peak is lower than ω_{ci0}. Figures 1(a) and 1(b) denote a central cell line density N_l and a central cell diamagnetic signal D. Since the electron temperature T_e is much smaller than $T_\perp$, the diamagnetic signal represents the perpendicular pressure of the hot ions. As the diamagnetic signal increases, an AIC mode is excited as shown in Fig. 1(c). The AIC mode is measured with a reflectometer installed near the midplane of the central cell. Simultaneously with AIC mode excitation, a steplike increase in the collector current of the energy analyzer is observed as depicted in Fig. 1(d). Here, the electron repeller voltage is kept constant, and the increase in the collector current indicates an increase in the end-loss current I_e flowing into the end plate.

The mean energy of the end-loss electrons also increases. Figure 2 denotes the collector currents just before and just after AIC mode excitation, plotted as functions of the electron repeller voltage of the energy analyzer. The energy distribution of the end-loss electrons can be fitted to a one component Maxwellian. The electron temperature as evaluated from the slope of the current-voltage curve slightly increases with excitation of the AIC mode. Figure 3 shows time variations of the diamagnetic signal, the electron current, and the electron temperature. As was point out above, I_e increases with AIC excitation but gradually decreases with time. A small increase in the electron temperature with AIC is also seen. As with I_e, T_e has a maximum value just after AIC excitation and decreases very slightly with time.

Axial heat flow to the end plate carried by electrons is roughly represented by $2T_eI_e$ [19]. It has been considered that, in a hot ion mode of GAMMA 10, the power source of electron heating is electron drag on hot ions. We then evaluate the end-loss power carried by electrons in terms of the electron drag power $P_{\text{drag}} = W_i/\tau_{\text{drag}}$ [20]. Here, W_i is the ion energy density and is well represented by D. The electron drag time is proportional to $T_e^{1.5}/n_e$. Thus $W_i/\tau_{\text{drag}} \propto N_{l^*}D/T_e^{1.5}$, assuming that the plasma radius does not change very much with time. Figure 4 plots $2T_eI_e$ as a function of $N_{l^*}D/T_e^{1.5}$. Before excitation of the AIC mode, as depicted by closed circles, the electron heat flow is very well proportional to the drag power. The AIC mode enhances the electron heat flow as shown by the open circles in Fig. 4. The value of $2T_eI_e$ becomes several times as large as the drag power. However, the electron heat flow gradually decreases with time and asymptotes to the level of the drag power. Although the time width of enhanced heat flow varies shot to shot, it is typically 10 through 20 ms. Thus the electron heat flow is enhanced transiently in the middle of ion heating and settles down to a value corresponding to the drag power.

The transient phenomenon of electron acceleration suggests a resonant interaction between electrons and the AIC mode. Electron Landau damping is a possible mechanism. The power absorbed by electrons in Landau damping is given by [5]

$$P_{\text{LD}} = \sqrt{\pi}\,\omega\varepsilon_0 E_\parallel^2 \left(\frac{\omega_{\text{pe}}}{\omega}\right)^2 \left(\frac{\omega}{k_\parallel v_e}\right)^3 \exp\left[-\left(\frac{\omega}{k_\parallel v_e}\right)^2\right]. \quad (1)$$

Here, ω is the wave frequency, ω_{pe} is the electron plasma

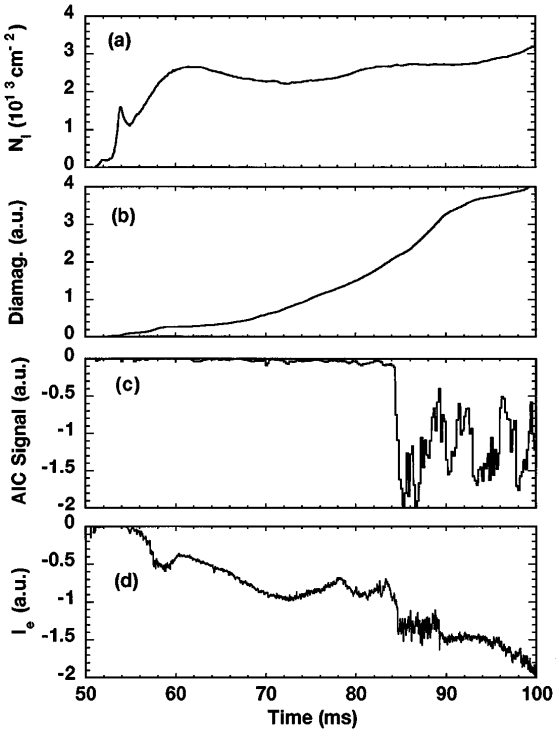

FIG. 1. Wave forms of the relevant parameters. (a) The line density of the central cell. (b) The central cell diamagnetic signal. (c) The AIC mode signal measured by a reflectometer. (d) The end-loss electron flux. In (c) and (d) the signals increase downward.

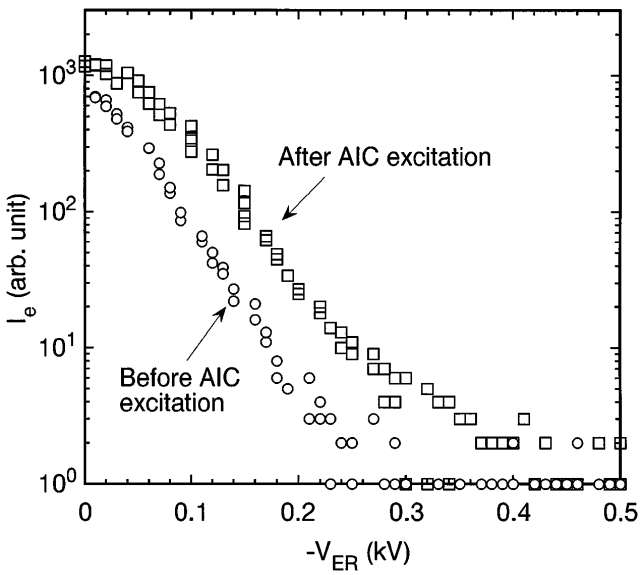

FIG. 2. Current-voltage curves of the end-loss electrons just before and just after onset of the AIC mode.

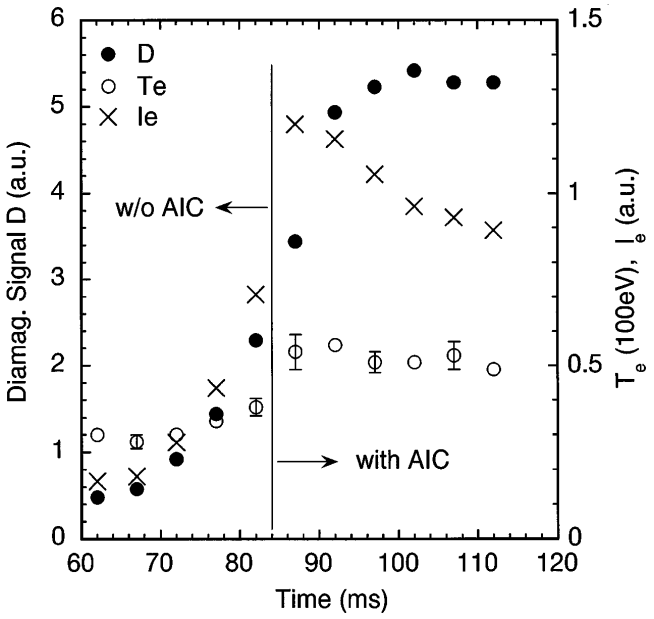

FIG. 3. Time variations of the diamagnetic signal, the end-loss electron flux, and the electron temperature are plotted by the closed circle, cross, and open circle, respectively.

frequency, $E_\parallel$ is the wave electric field parallel to the ambient magnetic field line, $k_\parallel$ is the parallel wave number, and v_e is the thermal velocity of electrons $v_e = (2T_e/m_e)^{1/2}$. Power absorption is maximum for $\omega/k_\parallel v_e = (3/2)^{1/2}$. This condition gives a relation $T_e(\mathrm{eV}) = 1.9 \times 10^{-12}(\omega/k_\parallel)^2$, ω in Hz and $k_\parallel$ in m^{-1}. Substituting the experimental values, $\omega \approx 2\pi \times 5.8$ MHz and $k_\parallel \approx 10\ \mathrm{m}^{-1}$, maximum coupling is expected for $T_e \approx 30$ eV. As shown in Fig. 3, the electron temperature is about 30 eV and meets this condition well.

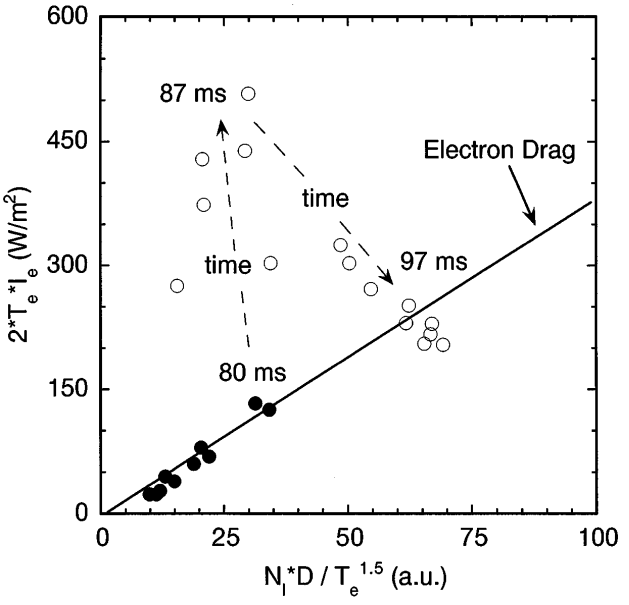

FIG. 4. The heat flow to the end plate is plotted as a function of $N_{i^*}D/T_e^{1.5}$. The horizontal axis is proportional to the electron drag power. The closed circle stands for the heat flow before excitation of the AIC mode and the open circle depicts that after excitation. The indicated times are representative values.

We then compare P_{LD} with P_{drag}. For $n_e = 2 \times 10^{12}\ \mathrm{cm}^{-3}$, $T_i = 2$ keV, and $T_e = 50$ eV, typical in the central cell of GAMMA 10, the drag power P_{drag} is estimated to be $1.7 \times 10^5\ \mathrm{W/m}^3$. For the same condition, the Landau damping power is evaluated to be $P_{\mathrm{LD}} \approx 1.1 \times 10^3 E_\parallel^2\ \mathrm{W/m}^3$. By using the parallel component of the Ampere law of the Maxwell equations $(\nabla \times B)_\parallel = \omega \varepsilon_0 \mu_0 \mathrm{K}_\parallel E_\parallel$, the magnitude of $E_\parallel$ is evaluated for a cold plasma as [21]

$$E_\parallel \approx \frac{c^2}{\omega}\left(\frac{\omega}{\omega_{\mathrm{pe}}}\right)^2 k_r B_\theta\,. \tag{2}$$

Here, k_r is the radial wave number and B_θ is the azimuthal component of the wave magnetic field. For $n_e \approx 2 \times 10^{12}\ \mathrm{cm}^{-3}$ and $k_r \approx 2\pi/a$ for a plasma radius a of about 0.1 m, the parallel electric field is given by $E_\parallel \approx 3.3 \times 10^4 B_\theta(\mathrm{T})\ \mathrm{V/m}$. The magnitude of B_θ is estimated from magnetic probes located near the midplane and near the mirror throat of the central cell [11,17]. The on-axis value of B_θ is evaluated to a factor of $\times 10^{-4}$ T, which gives $E_\parallel \geq 10\ \mathrm{V/m}$ [22]. Thus P_{LD} compares well with P_{drag}. This is consistent with the enhanced heat flux to the end plate, which is nearly double the drag power, as plotted in Fig. 4. The AIC mode has a significant amplitude in the central cell [11,16]. The region in which the electrons gain energy from hot ions is also limited to the central cell. Therefore, the comparison of P_{LD} with P_{drag} is valid. The Landau damping power depends on the electron velocity distribution [23]. Equation (1) assumes an isotropic electron distribution function. Frequent electron collisions ($\tau_e < 10\ \mu$s) keep the distribution isotropic in the present experiment.

One remarkable feature of the present observation is that enhancement of the end-loss electron flux lasts for only $\sim$10–20 ms after excitation of the AIC mode. Characteristics of the AIC mode are measured with magnetic probes. The AIC mode has several frequency peaks. Figure 5(a) shows time variations of the peak frequencies. After onset of the AIC mode, they shift slightly upward with time but they are bounded within a narrow frequency band and then gradually approach constant values. The value of ω_{ci0} is 6.16 MHz. Thus the peak frequencies lie in between $\sim 0.9\omega_{\mathrm{ci0}}$–$0.95\omega_{\mathrm{ci0}}$. The parallel wave number is estimated from the phase difference $\Delta\phi$ between the AIC signals detected on two magnetic probes installed near the midplane with an axial distance Δl. Figure 5(b) depicts $\Delta\phi/\Delta l$ corresponding to each frequency peak. Just after onset, the AIC mode is a traveling wave and finite $\Delta\phi/\Delta l$ of $\sim$5–10 m^{-1} corresponds to the parallel wave number $k_\parallel$. Although $\Delta\phi/\Delta l$ soon asymptotes to a very small value, a detailed examination indicates that the variation of $\Delta\phi/\Delta l$ is not due to a shift to a long wavelength side but is due to a change to a standing wave. The wavelength itself becomes rather short [16].

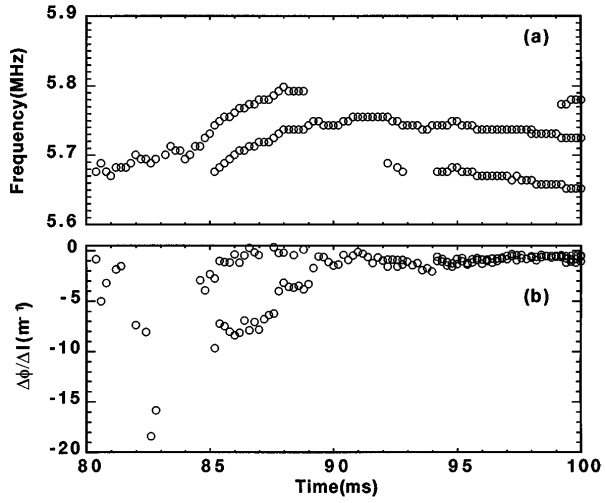

FIG. 5. Time variations of the frequencies of the AIC mode (a) and the parallel wave numbers corresponding to each frequency (b). The value of $k_\parallel$ is evaluated as $k_\parallel = \Delta\phi/\Delta l$. Here, $\Delta\phi$ is the phase difference between the magnetic fluctuations picked up by two magnetic probes placed with the axial distance Δl.

The transient increase in the heat flow is interpreted as follows. As is seen in Fig. 5(a), the frequency of the AIC mode is bounded in a narrow band and hence almost constant. Then, the power absorption by electrons P_{LD} is proportional to $x^3 \exp(-x^2)$, where $x = \omega/k_\parallel v_e$. Here, we assume constancy of the electron density [see Fig. 1(a)]. Thus P_{LD} is maximum at $x_0 = (3/2)^{1/2}$ and quickly falls for $x < x_0$ or $x > x_0$. Experimental parameters at the onset of the AIC mode, $T_e \approx 30$ eV and $k_\parallel \leq 10\ \mathrm{m}^{-1}$, are very close to the condition of maximum power absorption. This explains the jump of the heat flow to the end plate as plotted in Fig. 4. Subsequently, T_e increases and the wavelength of the AIC mode decreases with increasing frequency. This leads to a decrease in x and then results in a substantial decrease in P_{LD}. At a later time, x decreases to about 0.5, which results in a decrease in P_{LD} by about 70%. In the meantime, the drag power increases as the ion temperature increases, and the electron temperature of about 60 eV is sustained by electron drag only. The value of $k_\parallel$ sometimes takes a value at about $10\ \mathrm{m}^{-1}$ again at a later time, and the heat flow also increases at the same time. Moreover, when ion heating power is adjusted in order for the hot ion pressure to keep an appropriate value, $k_\parallel$ remains $5-10\ \mathrm{m}^{-1}$. In this case, the increase in the electron heat flow lasts for a long time.

The observations described so far strongly suggest that the electron acceleration is due to electron Landau damping of the AIC mode. Here, we enumerate the facts supporting this. First, the increase in the heat flow is triggered by the AIC mode and well accounted for by Eq. (1). Second, the enhancement of the heat flow resonantly occurs only for $x \approx x_0$. Third, the AIC mode is a spontaneously excited plasma wave and there is no possibility of electron acceleration due to a near field of an antenna. Moreover, since the electron collision frequency is much smaller than the AIC frequency ($\nu_{\mathrm{coll}} \approx \nu_{\mathrm{AIC}}/20$), collisional damping does not cause electron heating. The small collision frequency ensures the conditions of the validity of Landau damping [5].

In summary, we have observed enhancement of the end-loss electron flux and the heat flow to the end plate in GAMMA 10 during the phase of hot ion creation. This enhancement is driven by the AIC mode. The increase in the heat flow is equal to or higher than the electron drag power on hot ions. The present observation shows that electron Landau damping of the AIC mode is the most probable mechanism of the parallel electron acceleration.

The authors thank the members of the GAMMA 10 Group for their collaboration and valuable discussion during this work.

*Present address: Faculty of Integrated Human Studies, Kyoto University, Sakyouku, Kyoto, 606-8501, Japan.
†Present address: National Institute for Fusion Science, Toki, Gifu, 509-5259, Japan.

[1] T. H. Stix, Nucl. Fusion **15**, 737 (1975).
[2] N. J. Fish and C. F. F. Karney, Phys. Fluids **24**, 27 (1981).
[3] C. C. Petty *et al.*, Nucl. Fusion **35**, 773 (1995).
[4] T. Intrator *et al.*, in *Radio Frequency Power in Plasmas*, edited by R. Prater and V. S. Chan, AIP Conf. Proc. No. 355 (AIP, New York, 1996), p. 221.
[5] T. H. Stix, *Waves in Plasmas* (AIP, New York, 1992).
[6] F. F. Chen, Plasma Phys. Control. Fusion **33**, 339 (1991).
[7] A. W. Molvik, A. R. Ellingboe, and T. D. Rognlien, Phys. Rev. Lett. **79**, 233 (1997).
[8] R. T. S. Chen and N. Hershkowitz, Phys. Rev. Lett. **80**, 4677 (1998).
[9] T. Tamano, Phys. Plasmas **2**, 2321 (1995).
[10] M. Ichimura *et al.*, Phys. Rev. Lett. **70**, 2734 (1993).
[11] R. Katsumata *et al.*, Phys. Plasmas **3**, 4489 (1996).
[12] R. F. Post, Nucl. Fusion **27**, 1577 (1987).
[13] A. Roux *et al.*, J. Geophys. Res. **87**, 8174 (1982).
[14] S. Yoshikawa and H. Yamato, Phys. Fluids **9**, 1814 (1966).
[15] A. Mase *et al.*, Phys. Fluids B **5**, 1677 (1993).
[16] A. Kumagai *et al.*, Jpn. J. Appl. Phys. **36**, 6978 (1997).
[17] R. Katsumata *et al.*, Jpn. J. Appl. Phys. **31**, 2249 (1992).
[18] The reflectometer finds density and magnetic fluctuations in the microwave power returning from the cutoff layer as a reflection of an incident probe microwave. For more detail, see Ref. [15].
[19] T. Saito *et al.*, J. Phys. Soc. Jpn. **66**, 3809 (1997).
[20] J. Wesson, *Tokamaks* (Clarendon Press, Oxford, 1997).
[21] W. P. Allis, S. J. Buchsbaum, and A. Bers, *Waves in Anisotropic Plasmas* (MIT, Cambridge, MA, 1963).
[22] Since hot ions do not reach the mirror throat, the mirror throat magnetic probe can be inserted into the axis without disturbance. For the fluctuation amplitude, see also Ref. [15] and A. Mase *et al.*, [Rev. Sci. Instrum. **66**, 821 (1995)].
[23] M. Porkolab, in *Radio Frequency Power in Plasmas*, edited by Donald B. Batchelor, AIP Conf. Proc. No. 244 (AIP, New York, 1992), p. 197.